DYNAMIC ANALYSIS OF ADSORPTIVE HEAT TRANSFORMERS: OPTIMAL ADSORBENT

Yuriy I. Aristov

Boreskov Institute of Catalysis SB RAS
Lavrenieva Av., 5, Novosibirsk, 630090, RUSSIA
Email: aristov@catalysis.ru

Abstract

This paper presents a novel experimental method to study adsorption dynamics under conditions typical for an adsorptive heat transformer. Effect of the adsorbent nature, its grain size, residual non-adsorbable gas, heating rate, local shape of adsorption isobar on the adsorption dynamics and specific cooling (heating) power was studied for promising adsorbents of water (Fuji silica RD, FAM-Z02, SWS-1L). Based on these results some demands to an adsorbent optimal from the dynamic point of view have been discussed.

KEYWORDS

Adsorptive heat transformers Adsorption kinetics Optimal adsorbent Linear driving force model

INTRODUCTION

An adsorbent is a key element of adsorptive heat transformers, AHT (heat pumps, chillers and amplifiers) and its proper choice is of prime importance. Intelligent choice of adsorbent should be based on comprehensive analysis that takes into consideration both thermodynamic and dynamic aspects. Thermodynamic requirements to an optimal adsorbent which ensures the best cycle performance under prescribed operating conditions were reported for non-regenerative AHT cycles in [1, 2]. These requirements for a basic cycle reversibly operating at the fixed evaporator temperature T_e and condenser temperature T_c are based on an universal relation between three cycle temperatures (T_e, T_c and the minimal desorption temperature T_2) [3] $T_2 \cdot T_e = T_c^2$, that directly comes from the empiric Truton's rule [4] or the Polaniy principle of temperature invariance [5]. The conclusion was drawn that the optimal adsorbent should have a step-like adsorption isobar with the step positioned exactly at $T = T_2$ (at $P = P_o(T_c)$). Because of zero temperature difference between an adsorber and an external heat source the entropy generation is absent and the AHT efficiency can reach the Carnot efficiency [1, 6]. On the other hand, no driving force for heat transfer

Kinetic properties of the adsorbent strongly affect the dynamic behaviour of AHT and contribute to the specific power of the unit. This paper gives an overview of the current state of the art in this field and presents a novel approach focused on studying adsorption dynamics under conditions typical for AHT. This approach closely imitates boundary conditions of isobaric stages of AHT when adsorption (desorption) is initiated by a fast drop (jump) of the temperature of a heat exchanger (HE) wall which is in thermal contact with the adsorbent [6-11]. This method allowed experimental modelling the dynamics of isobaric stages of AHT. The effects of adsorbent nature, its grain size, heating rate, residual non-adsorbable gas, etc. on the uptake evolution and AHT specific power were experimentally examined for promising adsorbents (Fuji silica RD, FAM-Z02, SWSs). Applicability of the Linear Driving Force (LDF) model is discussed. Based on this method as well as on literature data some requirements to a dynamically optimal adsorbent and configuration of its layer are considered.

THE CURRENT STATE OF THE ART

As stated above, the adsorbent kinetic properties can strongly affect the dynamic behaviour of well-designed AHT and its specific power. Common way for taking these complex effects into account is a mathematical modelling of the AHT dynamics. These models are used for describing experimental behaviour of real AHT, predicting the performances, understanding the influence of the adsorbent properties, optimizing AHT operation, etc. Depending on the complexity, the dynamic models may be classified as lumped parameters (LP) and heat and mass transfer (HMT) models.

The HMT models take into account variation of the adsorbent temperature T_a, pressure P and adsorbate concentration *w* both in time and space. Hence, the governing equations are partial differential equations. The complex and nonlinear character of coupled heat and mass transfer requires sophisticated and time-consuming numerical methods for solving these equations and simulation of adsorbent bed dynamics. Because of this the HMT models are not wide-spread and the most popular are LP models which give a simplified representation of the adsorption process, neglecting any space gradients. The following assumptions are generally made: a) the temperature T_a is uniform in the adsorbent layer; b) the refrigerant (adsorbate, working fluid) is distributed in the adsorber uniformly and can be described by the average concentration *w*; and, c) the intrinsic adsorption is fast and at any time the equilibrium between solid and gas phases are attained. In the LP models only the heat transfer resistance between a HE wall and an adsorbent is considered, while that inside the adsorbent layer is neglected [12]. A common LP model includes three main equations representing the energy balance, mass balance and adsorption equilibrium. Such model was first applied for analysis of adsorptive chillers in [13, 14] and afterwards was replicated in both original or modified forms in many papers [15-22]. Only two dynamic characteristics of an adsorbent are presented in the LP equations: the adsorption rate d*w*/dt and the coefficient of heat transfer between the adsorbent and the HE wall h. To calculate d*w*/dt the authors of [13] used the LDF model

$$dw/dt = K(w_{eq} - w) \tag{1}$$

with the efficient rate constant

$$K(T) = 15D_{ef}(T)/R_p^2 , \tag{2}$$

where $D_{ef}(T) = D_{ef0} \exp(-E_a/RT)$ is the temperature dependent effective diffusivity, R_p is the radius of a spherical grain, w_{eq} and *w* are equilibrium and current uptakes. In [13] there was no special justification for applying Eq. (1), just a reference to Glueckauf [23] who first suggested it to simplify a numerical analysis of the sorption dynamics in chromatographic columns.

Determination of the effective diffusivity D_{ef}. To measure the water diffusivity (means, D_{ef0} and E_a) in a silica Fuji type A the authors of [13] applied the well known Isothermal Differential Step (IDS) method [24, 25]. This quasi-equilibrium method is considered to be reliable as it allows obtaining the diffusivity in the case of a non-linear adsorption isotherm [25]. The procedure based on the moderate deviation of the system "vapour-adsorbent" out of adsorption equilibrium by a small jump of the vapour pressure.

The adsorption kinetics was found to follow the Fickian Diffusion (FD) model [13]. The weight change was analyzed to obtain the water diffusivity D_{ef} by fitting of these experimental curves with the theoretical model [24]. So obtained diffusivities were approximated in [13] by the function $D_{ef} = D_{ef0} \exp(-E_a/RT)$ with $D_{ef0} = 2.54\ 10^{-4}$ m^2/s and $E_a = 42.0$ kJ/mol. These values allowed successful interpretation of the experimental results of [13] and were used in numerous later simulations [15-22]. Similar values for the Fuji silica type RD were measured by the IDS method in [26]: $D_{ef0} = 2.9\ 10^{-4}$ m^2/s and $E_a = 41.5$ kJ/mol. They are close to those for the silica Fuji type A, because these adsorbents have almost equal pore structure [26].

Determination of the heat transfer coefficient h. The heat transfer resistance 1/h between the HE wall and the adsorbent layer is a rate limiting factor in many AHTs, especially utilizing loose adsorbent grains. The heat transfer coefficient h can be estimated as follows [27]: if the main mechanism of heat transfer from the plate to the grain (or vice versa) is the heat conductance through the layer of a stagnant vapour, then $h \approx \lambda/R_p = 30\text{-}35$ W/(m^2·K), where $\lambda = 0.021$ W/(m·K) is the heat conductivity of water vapour at T = 70°C. A few experimental studies were dedicated to direct measurements of this important parameter [28]. This value was dependent on the gas nature and pressure and changed for Ar from 35 to 75 W/(m^2·R) and for He from 75 to 200 W/(m^2·R). The authors mentioned that this value increases for smaller grains with higher skeleton heat conductivity and smaller average bed porosity. Probably because of this complexity some confusion does exist in literature: for water vapour the heat transfer coefficient h of 15 to 50 W/(m^2·R) has been used by various authors [13-18, 29-32]. No reliable data on temperature dependence h(T) are available in literature, and in LP models h is as-

sumed to be constant. For vapours this resistance can be additionally affected by the heat pipe effect which was reported by Zhang and Wang [29] during the isosteric phases of AHT cycle. This creates an additional channel of the transfer due to a convective vapour flux towards colder sites in the adsorbent layer [22, 32] enhancing both heat and mass transfer.

Other input parameters should be measured and input in the LP models are the adsorbent specific heat $C_p(w)$ and the heat of adsorption $\Delta H_a(w)$ as well as some apparatus characteristics. If the thermodynamic and dynamic parameters are identified, the evolution of the temperature, pressure and concentration can be obtained by numerical solving a system of ordinary differential and algebraic equations. Hence, even simplified LP models require many experimental parameters to be known. Moreover, a serious obstacle is a reliability of these input parameters: the uncertainty with the h-values has been already mentioned. Let us consider another fundamental discrepancy of the current methodology: the values of D_{ef} and h measured under quasi-equilibrium conditions can be quite different from those at real conditions of AHT cycle. Indeed, for the IDS method the adsorption driving force is a small pressure jump, and thermal effects can be neglected, whereas at common AHTs the adsorption is initiated by a large drop of the temperature of a metal support (HE fins) at a constant pressure over the adsorbent.

NEW METHODOLOGY OF STUDYNG AHT DYNAMICS

Adsorption dynamics under real conditions of AHT. To avoid the mentioned fundamental discrepancy of the current methodology we suggested [6] a new Large Temperature Jump (LTJ) method to study the dynamics of refrigerant adsorption (desorption) under conditions which almost repeat the isobaric stages of AHT cycle. The measurements were performed with one layer of loose adsorbent grains placed on a metal plate which imitates a HE fin (Fig. 1). Temperature of the plate was changed due to a thermal carrier circulating under the plate. Vapour pressure over the adsorbent was main-tained almost constant by connecting the measuring cell to a large vapour vessel which moderated the pres-sure change. Water uptake was converted from the pressure evolution P(t). This method allows a direct measurement of adsorption dynamics under conditions, which closely simulate the scenario of temperature jump or drop in real AHT.

Experimental setup contained three main compartments: the measuring cell, the vapour vessel and the evaporator (Fig. 2). Loose adsorbent grains (mass 150-400 mg) were placed in one layer on a metal holder. Its temperature could be adjusted and controlled with the accuracy of ±0.1ºC using a heat carrier circuit coupled by a three-way valve (3WV) either to circulating

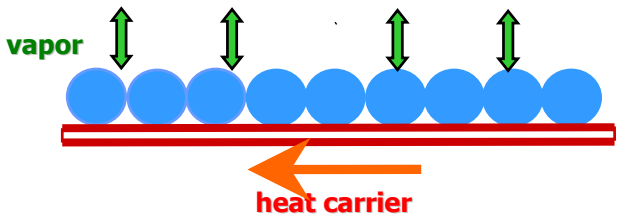

Fig. 1. Schematic of the layer configuration

thermal bath 1 or 2. The vapour pressure was measured by an absolute pressure transducer MKS Baratron® type 626A (accuracy ±0.01 mbar). More experimental details can be found elsewhere [6, 8, 10, 11]. This set-up was a modification of the constant-volume, variable pressure setup first suggested by Knocke [33] and then applied in [34]. That approach can be called as a Large Pressure Jump (LPJ) method as the driving force for water adsorption was a large jump of the pressure over the adsorbent.
Typical adsorption LTJ run was as follows [6]. A monolayer of loose adsorbent grains was heated to the starting temperature of the isobaric adsorption stage T_0 = 60 ºC and evacuated for two hours using a vacuum pump (valves V_{MC}, V_2, V_3 were opened, V_A & V_1 was closed). Then the vapour vessel and the measuring cell were connected to the evaporator and the starting pressure of the adsorption process, e.g. $P_{ev}(T_e$ = 10 ºC) = 12.4 mbar was set (V_1, V_{MC} & V_3 were open, V_2 & V_A were closed). The sample was equilibrated with water vapour for two hours. After that valve V1 was closed and the metal holder was cooled down to T_f = 35 ºC by turning 3WV (V_{MC} was open). It initiated the adsorp-

tion process and the vapour pressure over the adsorbent was reduced by some 1.5-2.5 mbar, so that the process could be considered as quasi-isobaric. To initiate the desorption run the reverse temperature leap was performed. Data on the pressure evolution P(t) required for calculating the water uptake $\Delta m_{H2O}(t)$ were recorded each 1 s by a data acquisition system.

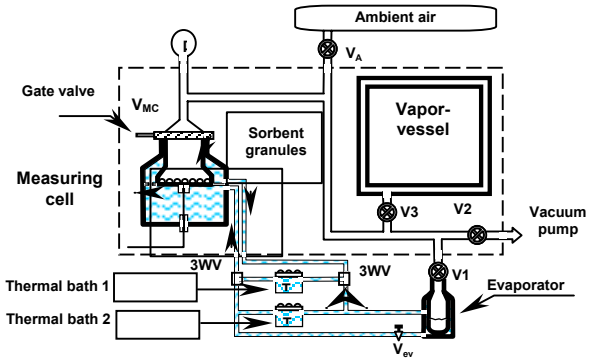

Fig. 2. Schematic diagram of the LTJ kinetic setup

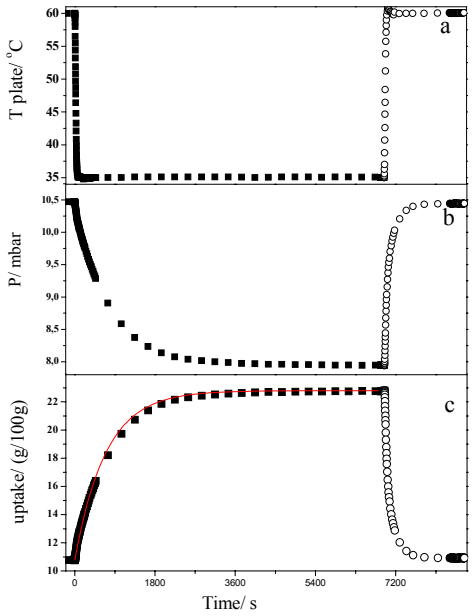

Fig. 3. Temperature evolution of metal plate (a), pressure over the sample (b) and the water uptake (c) for cooling (bold symbols) and heating (open symbols) runs for SWS-1L grains (size 0.8–0.9 mm). The solid line is exponential approximation $m_t = m_0+(m_f - m_0)(1–\exp(-t/\tau))$ [10]

Typical evolution of the temperature of the metal plate, the vapour pressure over the sample and the water uptake are shown on Fig. 3 for the composite SWS-1L ("$CaCl_2$ in the KSK silica pores"). After initiating the cooling process, the holder reached the final temperature T_f for app. 1 min (Fig. 3 a), while the pressure reduction was slower and completed within some tens minutes (Fig. 3 b). Hence, the adsorption took place at almost constant temperature of the holder equal to its final temperature as it was considered in the mathematical model described in [7]. Near-exponential evolution of the uptake *w* on time was found for both adsorption and desorption runs (Fig. 3 c).

The LTJ method was further applied to study effects of adsorbent nature, its grain size, heating rate, residual non-adsorbable gas, etc. on the uptake evolution and AHT specific power. The experiments have been run on loose grains of water adsorbents promising for AHT, namely, Fuji silica RD (Fuji Silysia Ltd.) [26], FAM-Z02 (Mitsubishi Chemical Ltd.) [35] and SWS-1L.

Adsorbent nature. The new LTJ methodology allows a simple and reliable comparison of various adsorbents to be used in AHTs. For the three mentioned adsorbents evolution of the dimensionless water uptake in time is presented in Fig. 4 a for typical conditions of isobaric adsorption stage. It takes 101, 307 and 453 s to reach 80 % of the equilibrium uptake for silica, SWS-1L and FAM-Z02, respectively. Absolute variation of the uptake was 0.094, 0.176 and 0.206 g/g (Fig. 4 b), that gives the specific cooling power of 2.3, 1.4 and 1.1 kW/kg. At short adsorption time all the adsorbents generate almost the same cooling power (Fig. 4) exceeding 2.3 kW/kg. Hence, even simplest configuration of adsorbent bed - a single layer of touched adsorbent grains loosely placed on the metal plate [36] – can combine easy realization with practically attractive cooling power.

For silica and SWS, the experimental uptake curves were close to exponential, while for FAM a long tail was observed at the uptakes larger than 0.8 (Fig. 4 a). This is probably caused by FAM structural transformations.

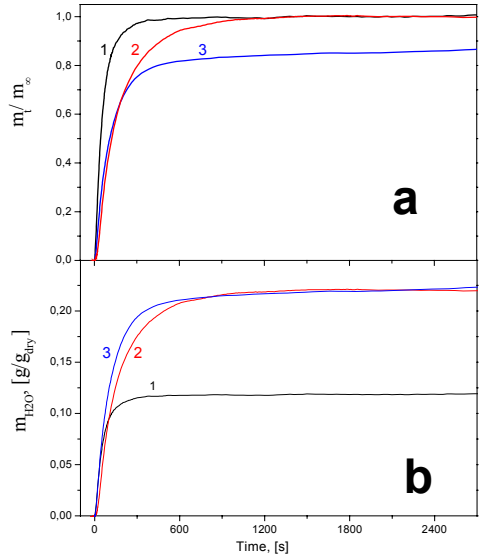

Fig. 4. Dimensionless (a) and absolute (b) adsorption uptake curves for loose grains 0.8–0.9 mm size, initiated by a temperature jump 60 °C=>35 °C: *1* – Fuji RD, *2* – SWS 1L, *3* – FAM-Z02. $P^0_{H_2O}$ = 10.3 mbar

Grain size. The size of adsorbent grains can affect simultaneously both heat and mass transfer in the adsorbent bed. Adsorption was faster for smaller grains (Fig. 5). The shape of these kinetic curves was near-exponential over the range 0÷90 % of the final uptake while the tail was longer than exponential. The times $\tau_{0.5}$ and $\tau_{0.8}$ corresponding to 50 and 80 % of the final uptake were found to be 2 ÷ 15 min. that is reasonable for practice (Fig. 5). For larger grains the ratio $\tau_{0.5}^{1.5mm} / \tau_{0.5}^{0.85mm}$ was close to $\left(r^{1.5\,mm} / r^{0.85mm}\right)^2$ that may indicate an essential contribution of intraparticle vapour diffusion to the total adsorption rate [10]. For smaller SWS grains the time of adsorption became very short and comparable with the time of the holder heating, so that the heat transfer seemed to play a dominant role. Strong acceleration of sorption process with the decrease in the FAM grain size was found in [8], too.

Residual air. From practical experience it is known that some amount of a non-adsorbing gas such as air can "poison" two-phase heat and mass transfer, reducing adsorption rate. The LTJ approach allows careful study of this effect [10]. We found that the presence of air at the partial pressure as low as 0.06 mbar can visibly decrease the rate of water adsorption by SWS-1L (Fig. 6). It was especially significant at the intermediate uptakes $0.3 < m_t/m_f < 0.9$, while at smaller and larger uptakes no influence was revealed (Fig. 6). The reduction of the adsorption rate can be caused by the Stephan flux which effectively sweeps air to the grain surface where it accumulates as an air-rich layer [37]. The transfer of vapour to the surface may then become controlled by the diffusion through this layer. At small uptakes this layer, probably, did not have enough time to form. At large uptakes ($m_t/m_f > 0.95$) adsorption rate is low and the Stephan flux was not sufficient to efficiently sweep air to the grain surface, hence, the

extra-resistance was small. It was not unlikely that the residual air can also accumulate inside the grain pores so that the combined effect of external and internal resistances took place.

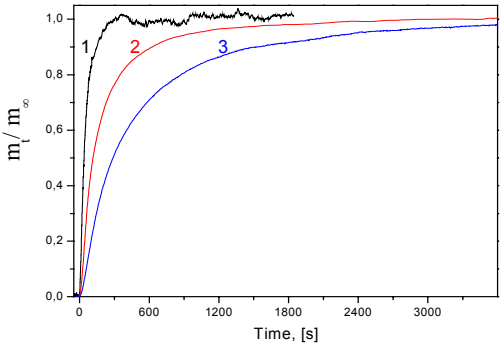

Fig. 5. Adsorption dynamics for loose SWS-1L grains initiated by temperature jump 60 => 35 °C at various grain size: *1* – 0.355–0.425 mm, 2 – 0.8–0.9 mm and 3 – 1.4–1.6 mm.

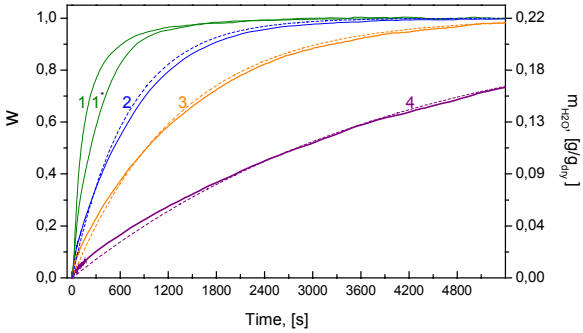

Fig. 6. Inhibition of the adsorption rate for SWS-1L grains 0.8–0.9 mm in the presence of air. 1) $P_A \le 0.02$ mbar; 1*) $P_A = 0.06$ mbar; 2) $P_A = 0.4$ mbar; 3) $P_A = 1$ mbar; 4) $P_A = 4.7$ mbar. Dotted lines – exponential approximation

Experimental kinetic curves were near-exponential $m_t = m_0 + (m_f - m_0)\cdot(1–\exp(-t/\tau))$. At $P_A \ge 0.4$ mbar the characteristic time of adsorption was $\tau = \tau_0 + BP_A$, where $B = 700 \pm 50$ s/mbar for the both grain sizes [10, 11]. Similar linear dependences were observed for Fuji RD and FAM-Z02, although an inhibition of the sorption rate was less strong than for SWS (Fig. 7). Hence, a careful removal of non-adsorbable gases from the adsorbent surface, set-up walls and degassing water in the evaporator is strictly obligatory prior a start-up of an AHT.

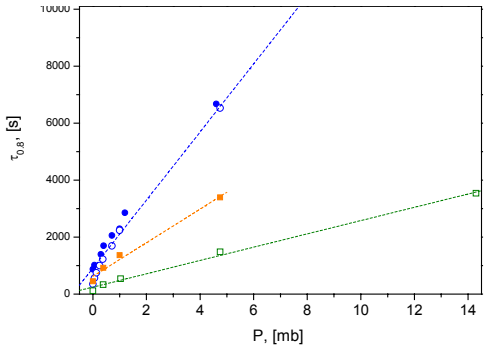

Fig. 7. Characteristic adsorption time $\tau_{0.8}$ as a function of air pressure for SWS-1L (• – 1.4–1.6 mm and o – 0.8–0.9 mm), silica Fuji (□ – 0.8–0.9 mm) and FAM-Z02 (■ – 0.8–0.9 mm). Dotted lines – linear approximation $\tau = A + B*P$

Heating rate. For the fast heating run the metal plate became isothermal in 50-100 s, while for the slow one, it took 300 s and 500 s for the heating and cooling, respectively (Fig. 8). As a result, the uptake changed much slower than for the fast run. Especially large difference was observed at the initial part of uptake curve, which was rather S-shaped than exponential (Fig. 8 c). To analyse such complex kinetics we introduced the characteristic times $\tau_{0.5}$ and $\tau_{0.9}$. The $\tau_{0.5}$-time was much longer for the slow temperature change, while the $\tau_{0.9}$-times were almost equal, especially for cooling mode [6]. Thus, a cooling scenario affects the beginning of uptake curve stronger than its tail.

Specific power. For the exponential uptake curves the instantaneous specific power W(t) which is consumed (released) in the evaporator (condenser) is $W = H\,(dm/dt)/m_a = W_{max}\exp(-t/\tau)$, where H is the latent heat of evaporation of liquid water taken as 2478 J/g, m_a is the mass of dry adsorbent, $W_{max} = \Delta H\,(m_\infty – m_o)/(\tau\, m_a)$ is the maximum specific power at $t \Rightarrow 0$. Even for quite large SWS grains (1.4-1.6

mm) at heating stage it could reach 3.7 kW/kg at the vapour pressure 55-60 mbar. For water adsorption at low vapour pressure (10-15 mbar) the maximum power was still good (0.75-1.9 kW/kg).

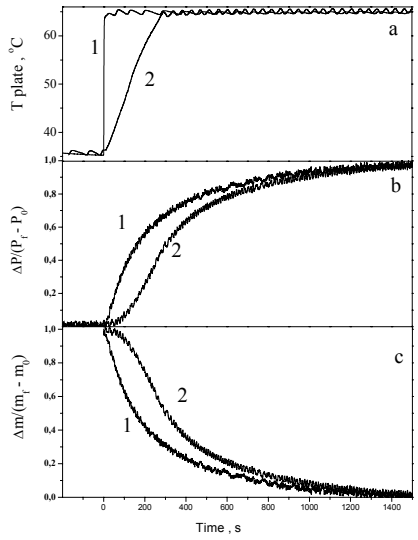

Fig. 8. Temperature evolution of the metal plate (a), the pressure over the sample (b) and the water uptake (c) for different heating scenario: 1 – fast and 2 – slow [6]

Thus, our LTJ tests with loose adsorbent grains give experimental evidence for the possibility to build quite compact adsorption cooling/heating devices which utilize loose grains of Fuji RD, FAM-Z02 and SWS-1L. One can expect even higher specific power for a compact adsorbent layer prepared with a binder and consolidated with metal surface of heat exchanger [28]. The measured uptake curves were exponential, that can be formally obtained by integrating Eq. (1). On the one hand, this justifies applicability of the LDF model for analyzing isobaric stages of AHT cycles as it was suggested in [13, 14]. On the other hand, the exponential shape of the uptake curves can be derived from Eq. (1) only at K = const but not at K dependent on T as ordered in [13, 23] (Eq. (2)). It means that calculations with LP models for the studied configuration of adsorbent layer can be simplified by using a constant K instead of that introduced by Eq.(1). Indeed, for the configuration of the system "adsorbent-HE" and fast heating conditions discussed above, dynamics of each isobaric stage of AHT cycle can be unambiguously characterized by a single K-value. For particular case, K depends on the boundary temperatures T_o, T_f and grain size R_p and remains constant during adsorption (desorption) stage. Consequently, for fixed cycle this value can be directly measured and then introduced into heat and mass balance equations. Then a simple analytical expression can be easily obtained for the derivative dw/dt. In fortunate fact, a near-constancy of K and, hence, a simple exponential shape of experimental kinetic curves is a result of a complex interference of HMT processes in the system "HE wall – adsorbent". Although K implicitly depends on D_{ef} and h, no exact knowledge of these coefficients and their temperature dependence is necessary any more for making dynamic calculations. Models based on constant K can be called as "super-lumped parameter" models.

This approach can be generalized to any given configuration of the "HE-adsorbent" system. Indeed, if the uptake w(t) has been directly measured for the particular configuration (or for representative piece of this configuration), then, the adsorption rate dw/dt can be obtained by a numerical differentiation of the experimental function w(t) and can be immediately input in a LP model instead of Eq. (2) or any other simplification.

Mathematical model of the coupled heat and mass transfer under the LTJ run. For deeper understanding a coupled heat and mass transfer in the course of LTJ experiment a detailed HMT model was developed in [7]. A single adsorbent grain in thermal contact with a metal plate subjected to a fast temperature jump/drop at constant pressure was considered. The model took into account coupled heat and mass transfer in the grain with adsorption processes. Heat and mass transfer in a single adsorbent grain was described by detailed energy and mass balance equations [7]. This model was used for analysing the experimental results presented in [6] and for understanding links between dynamics and equilibrium parameters of adsorption process. The local adsorption equilibrium in each point of the

grain was assumed. The system of differential equations was numerically solved by methods of runs and iterations to obtain distributions of temperature T(r, t) and concentration in gas $C_w(r,t)$ and adsorbed w(r, t) phases.

Analysis of the experimental data. Good agreement between experimental and calculated uptake curves was obtained with the best fit corresponding to the efficient pore diffusivity $D = 3.0 \cdot 10^{-6}$ m^2/s and the efficient coefficient of heat transfer h = 120 W/(m^2·K). This diffusivity is very close to the Knudsen diffusivity in a straight cylindrical pore of radius r_p = 7.5 nm [25] at T = 90 °C = 363 K: $D_{kn} = 9700\, r_p \sqrt{T/\mu} = 3.3 \cdot 10^{-6}$ m^2/s. The diffusivity found in [7] is significantly higher than measured by the IDS method under isothermal conditions (T = 35-70 °C) for loose grains of SWS-1L [26]. The coefficient of heat transfer h obtained is also much larger than the one (15-60 W/(m·K)) commonly used. These differences in D and h indicated that at large deviations from the equilibrium the transfer of both heat and vapour ***can be more efficient*** than under quasi-equilibrium conditions. Possible reason could be an additional channel of the transfer due to a non-uniform temperature distribution that causes convective vapour flux towards colder sites in the system (a so called "heat pipe" or "recondensation" effect [22, 32]), which can enhance both heat and mass transfer.

The experimental and calculated characteristic times τ_c were in close agreement [7], hence the model accounted for major features of the LTJ experiments reported in [6]. In particular, the model confirms the quasi-exponential shape of the uptake curves, and the finding that the adsorption process was slower than the desorption one at the same temperature jump (Fig. 9). Moreover, our numerical calculations showed that the latter conclusion is not general and holds true only for particular conditions of temperature jumps applied in [6].

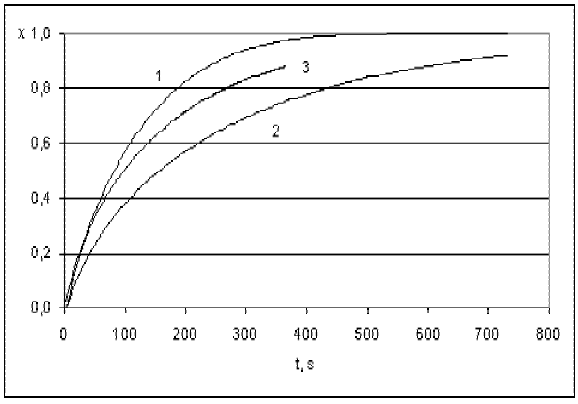

Fig. 9. Dimensionless uptake vs. time for a concave isobar (taken for SWS-1L): desorption (1) and adsorption (2). 3 – adsorption and desorption runs calculated for linear isobar. Jump 90°C ⇔ 80°C [7]

The interdependence between the heat and mass transfer can be more clearly seen if present the evolution of the grain state as "the average grain temperature T" vs. "the average pressure inside the grain P_w" (Fig. 10): **A** corresponds to the state of the system before the jump 90 °C ⇒ 80 °C. Line **ABD** represents the process of the grain cooling which initiates the adsorption of vapour. **D** corresponds to the state of the system before the jump 80 °C ⇒ 90 °C. Line **DEA** represents the process of the grain heating which initiates the desorption of vapour.

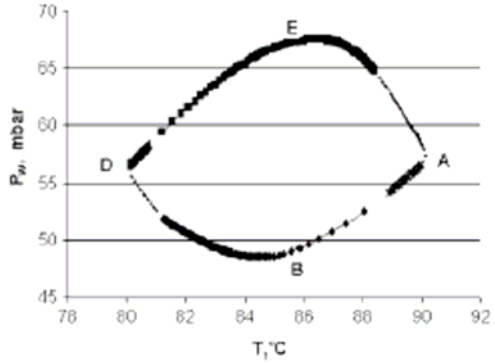

Fig. 10. Evolution of the average grain temperature T and the average pressure inside the grain P_w for the temperature jumps 90°C ⇔ 80°C [7]

For jump 90 ^{o}C $\Rightarrow$ 80 ^{o}C at t = 0 (point A) the driving force for heat transfer is maximum while the driving force for mass transfer equals 0. This initiates the fast cooling of the grain that reduces the driving force for the heat transfer. Dropping the grain temperature stimulates the adsorption of water molecules first from the gas phase inside the pores. As the adsorption is fast, at short times the diffusional flux of vapour into the grain is not sufficient to compensate the pressure decrease. The pressure difference P - P_w generates the driving force for mass transport which is increasing till point B (Fig. 10). The adsorption of water results in the release of the adsorption heat inside the grain which slows down the temperature decrease and so on. Thus, the mass and heat transfer processes are inevitably coupled and strongly affect each other. At longer times, P_w is increasing due to the vapour flux from the outside into the grain, until the system reaches the equilibrium at point D. At this point the driving forces for both the heat and mass transfer become zero. Similar evolution was observed during the reverse jump 80^{o}C $\Rightarrow$ 90^{o}C [7].

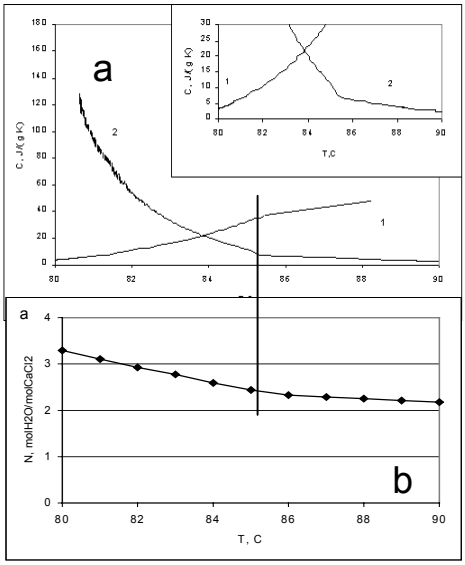

Fig. 11. Specific heat of an SWS-1L grain (a) as a function of the average temperature (1 – desorption, 2 – adsorption), isobar of water sorption (b) on SWS-1L at P = 56.5 mbar

The calculated specific heat C = dQ/dT/M of the grain as a function of the average grain temperature has a break at T $\approx$ 85.5^{0}C for both the adsorption and desorption runs (see the fragment on Fig. 11a) [7]. It is interesting that at the same temperature there is a break of the isobar *w*(T) of water sorption on SWS-1L (Fig. 11 b) at 56.5 mbar that is the average pressure during the jump. One can assume that these two breaks are linked. Indeed, during the desorption run the majority of water is desorbed within the temperature range from 80.0 to 85.5 ^{o}C, so that the heat needed for desorption is contributed to the large value of C (up to 160 J/(g·K)). At T > 85.5 ^{0}C the contribution of water desorption becomes much smaller; the C(T) has the break and is slowly approaching the sensible specific heat of the system (SiO_2+$CaCl_2$·$2H_2O$). During the adsorption run within the temperature range from 90.0 to 85.5 ^{o}C there is almost no adsorption (d*w*/dT is very small), and the average grain temperature changes faster than during reverse desorption run. At T^{av} < 85.5 ^{o}C the adsorption starts, because the absolute value of the derivative d*w*/dT increases. When T^{av} is approaching 90 ^{o}C the driving force for the heat transfer proportional to ΔT = (90 ^{o}C - T^{av}) is getting smaller, while [d*w*/dT] is continuously rising. This concave shape of adsorption isobar is the main reason why the adsorption has longer tail that desorption, that results in larger characteristic times. A linear sorption isobar leads to equal kinetics of adsorption and desorption (Fig. 9, curve 3), while convex isobar shape results in faster adsorption run. The latter has recently been confirmed experimentally [38].

Thus, a correlation between the driving force for heat transfer and the derivative d*w*/dT which defines the heat demand for desorption or heat release during adsorption, is dominant for overall dynamics in the LTJ runs as well as in real AHT. Since this driving force is gradually reducing, the derivative should decrease when T is approaching T_f, too. Hence, d^2w/dT^2 has to be negative. It means that to shorten the isobaric stages, at desorption run the isobar has to be concave while at adsorption

run – convex (Fig. 12).

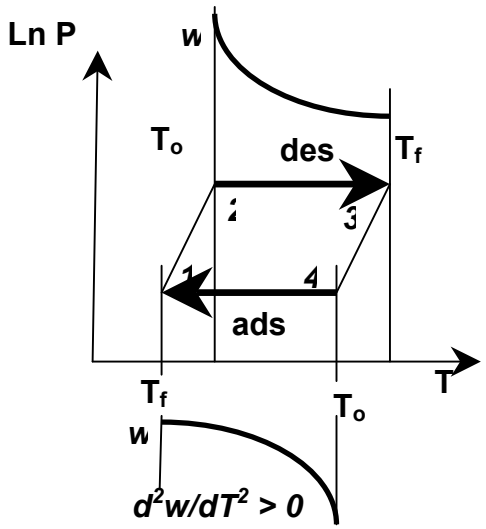

Fig. 12. Optimal shape of isobars at adsorption (4-1) and desorption (2-3) phases

Thus, the dynamics of water adsorption on a single adsorbent grain is closely linked with equilibrium properties of the adsorbent, in particular, with the shape (convex, concave or linear) of the segment of water adsorption isobar between the initial and final temperatures.

CONCLUSIONS

A novel experimental approach (LTJ) to study adsorption dynamics under conditions typical for AHTs has recently been suggested. It provides a correct methodology to investigate the effect of the adsorbent nature, its grain size, non-adsorbable gas, heating rate, shape of adsorption isobar, etc. on the adsorption dynamics. The main findings are a) near-exponential kinetic curves were found for a majority of adsorption and desorption runs, b) simple configuration of loose adsorbent grains can provide cooling power of 0.5-2 kW/kg; b) strong reduction of the adsorption rate in the presence of residual air; c) validity of the LDF model with a fixed rate constant; d) strong link between kinetic and equilibrium parameters. Mathematical modelling indicated that at large deviations from the equilibrium the transfer of both heat and vapour can be more efficient than under quasi-equilibrium conditions. Based on these results some demands to an adsorbent optimal from the dynamic point of view have been discussed.

Acknowledgements

The author thanks the Russian Foundation for Basic Researches for partial financial support of this study (grants 08-08-00808, 03-05-34762 and 08-08-90016).

Nomenclature

A	constant, s
B	constant, s/mbar
c	specific heat, J/(kg·°C)
D	diffusivity, m^2/s
E	activation energy, J/mol
h	heat transfer coefficient, $W/(m^2 \cdot °C)$
H	enthalpy, J/mol
K	rate constant, 1/s
m	mass, kg
P	pressure, mbar
r	pore radius, m
R	grain radius, m; universal gas constant, J/(m·K)
T	temperature, K, °C
t	time, s

w	adsorbate concentration, g/g
W	specific power, kW/kg
μ	molar mass, g
τ	characteristic time, s
Δ	increment
Subscripts	
a	adsorbent, activation
A	air
c	condenser
e	evaporator
ef	effective
eq	equilibrium
f	final
kn	Knudsen
max	maximum
p	particle; pore; at constant pressure
t	temporal
0	initial
∞	infinity

References

1. Aristov Yu. I. An optimal sorbent for adsorption heat pumps: thermodynamic requirements and molecular design // *Proc. VI Intern. Seminar "Heat pipes, heat pumps, refrigerators",* 12-15 Sept. 2005, Minsk, Belorus, pp. 342-353.
2. Aristov Yu. I. Novel materials for adsorptive heat pumping and storage: screening and nanotailoring of sorption properties // *J. Chem. Engn. Japan*, 2007, Vol. 40, pp. 1241-1251.
3. Critoph R. E. Performance limitation of adsorption cycles for solar cooling // *Sol. Energy*, 1988 Vol. 41, pp. 21-33.
4. Alefeld G., Radermacher R. *Heat Conversion Systems*, CRC Press, Boca Raton, 1994.
5. Aristov Yu. I., Sharonov V. E., Tokarev M. M. Universal relation between the boundary temperatures of a basic cycle of sorption heat machines // *Chem. Engn. Sci.*, 2008, Vol. 63, pp. 2907-2912.
6. Aristov Yu. I., Dawoud B., Glaznev I. S., A. Elyas A. A new methodology of studying the dynamics water sorption/desorption under real operating conditions of adsorption heat pumps: Experiment // *Intern. J. Heat and Mass Transfer*, 2008 (doi:10.1016/j. ijheatmasstransfer.2007.10.042).
7. Okunev B. N., Gromov A. P., Heifets L. I., Aristov Yu. I. A new methodology of studying the dynamics of water sorption/desorption under real operating conditions of adsorption heat pumps: Modelling of coupled heat and mass transfer // *Intern. J. Heat and Mass Transfer* , 2008, Vol. 51, pp. 246-252.
8. Dawoud B. On the effect of grain size on the kinetics of water vapour adsorption and desorption into/ from loose pellets of FAM-Z02 under a typical operating condition of adsorption heat pumps // *J. Chem. Engn. Japan* , Vol. 40, pp. 1298-1306.
9. Okunev B. N., Gromov A. P., Heifets L. I., Aristov Yu. I. Dynamics of water sorption on a single adsorbent grain caused by a pressure jump: modelling of coupled heat & mass transfer // *Int. J. Heat & Mass Transer* (doi:10.1016/j.ijheatmasstransfer.008.01.037).
10. Glaznev I. S., Aristov Yu. I. Kinetics of water adsorption on loose grains of SWS-1L under isobaric stages of adsorption heat pumps: the effect of residual air // *Int. J. Heat&Mass Transfer* (accepted).
11. Glaznev I. S., Ovoshchnikov D. S., Aristov Yu. I. Dynamics of water adsorption on loose grains in the presence of non-adsorbable gas under typical operating conditions of an adsorptive chiller, Cryogenics and Refrigeration // *Proc. ICCR'2008*, Shanghai, China, April 5-9, 2008, pp. 570-574.
12. Yong L., Sumathy K. Review of mathematical investigation on the closed adsorption heat pump and cooling systems // *Renewable and Sustainable Energy Reviews*, 2002, Vol. 6, pp. 305-337.
13. Sakoda A., Suzuki M. Fundamental study on solar powered adsorption cooling system // *J. Chem. Engn. Japan*, 1984, Vol. 17, pp. 52-57.

14. Sakoda A., Suzuki M. Simultaneous transport of heat and adsorbate in closed type adsorption cooling system utilizing solar heat // *J. Solar Energy Engin., Trans. of the ASME*, 1986, Vol. 108, pp. 239-245.
15. Douss N., Meunier F. Effect of operating temperatures on the coefficient of performance of active carbon-methanol systems // *J.Heat Recovery Systems & CHP* , 1988, Vol. 8, pp. 383–392.
16. Cho S.-H., Kim J.-N. Modelling of a silica gel/water sorption-cooling system // *Energy*, 1992, Vol. 17, pp. 829-839.
17. Saha B. B., Boelman E. C., Kashiwagi T. Computer simulation of a silica gel-water adsorption refrigeration cycle – The influence of operating conditions on cooling output and COP // *ASHRAE Transactions: Research*, 1995, Vol. 101, pp. 348-357.
18. Saha B. B., Boelman E. C., Kashiwagi T. Computational analysis of an advanced adsorption-refrigeration cycle // *Energy*, 1995, Vol. 20, pp. 983–994.
19. Critoph R. E. Forced convection adsorption cycles. // *Applied Thermal Engineering*, 1998, Vol. 18, pp. 255–269.
20. Cacciola G., Hajji A., Maggio G., Restuccia G. Dynamic simulation of a recuperative adsorption heat pump // *Energy*, 1993, Vol. 18, pp. 1125–1137.
21. Sami S.M., Tribes C. An improved model for predicting the dynamic behaviour of adsorption systems // *Applied Thermal Engineering* , 1996, Vol. 16, pp. 149–161.
22. Wu J. Y., Wang R. Z., Xu Y. X. Dynamic simulation and experiments of a heat regenerative adsorption heat pump // *Energy Conversion and Management*, 2000, Vol. 41, pp.1007–1018.
23. Glueckauf E. Part 10. Formulae for diffusion into spheres and their application to chromatography // *Trans. Faraday Soc.* 1955, Vol. 51, pp. 1540-1551.
24. Crank J. Mathematics of Diffusion, Oxford University Press, London, 1975.
25. Ruthven D. M. Principles of adsorption and adsorption processes, John Wiley&Sons, New York, 1984.
26. Aristov Yu. I., Tokarev M. M., Freni A., Glaznev I. S., Restuccia G. Kinetics of water adsorption on silica Fuji Davison RD // *Microporous & Mesoporous Materials*, 2006, Vol. 96, pp. 65-71.
27. Andersson J. Y., Bjurstroem H., Azoulay M., Carlsson B. Experimental and theoretical investigation of the kinetics of the sorption of water vapour by silica gel // *J. Chem.Soc., Faraday Trans.*, 1985, Vol. 1, № 81, pp. 2681-2692.
28. Guilleminot J. J., Gurgel J. M. Heat transfer intensification in adsorbent beds of adsorption thermal devices // *Proc. Intern. Solar Energy Conf. ASME*, Miami, USA, April 1990, pp. 69-74.
29. Zhang L. Z., Wang L., Momentum and heat transfer in the adsorbent of a waste-heat adsorption cooling system // *Energy*, 1999, Vol. 24, pp. 605-624.
30. Marletta L., Maggio G., Freni A., Ingrasciotta M., Restuccia G. A non-uniform temperature non-uniform pressure dynamic model of heat and mass transfer in compact adsorbent beds // *Int. J. Heat Mass Transfer*, 2002, Vol. 45, pp. 3321–3330.
31. Saha B. B., Chakraborty A., Koyama S., Aristov Yu. I. A New Generation Cooling Device Employing $CaCl_2$ -in-Silica gel–Water System // *Intern. J. Heat Mass Transfer*, 2008, (accepted).
32. Heifets L. I., Predtechenskaya D. M., Pavlov Yu. V., Okunev B. N. Modelling of dynamic effects in the adsorbent beds. 1. Simple method to estimate thermal conductivity of the composite adsorbent bed ($CaCl_2$, impregnated into pores of silica gel lattice) // *Moscow University Chemistry Bulletin*, 2006, Vol. 61, pp. 274-276.
33. Strauss R., Schallenberg K., Knocke K.F. Measurement of the kinetics of water vapour adsorption into solid zeolite layers // *Proc. Int. Symp. Solid Sorption Refrigeration*, Paris, November 18-21, 1992, pp. 227-231.
34. Dawoud B., Aristov Yu. I. Experimental study on the kinetics of water vapour sorption on selective water sorbents, silica-gels and alumina under typical operating conditions of sorption heat pumps // *Intern. J. Heat & Mass Transfer*, 2003, Vol. 46, pp. 273-281.
35. Kakiuchi H. M., Iwade S., Shimooka S., Ooshima K., Yamazaki M. and Takewaki T. "Water Vapour Adsorbent FAM-Z02 and Applicability to Adsorption Heat Pump" // *Kagaku Kogaku Ronbunshu*, 2005, Vol. 31, pp. 273-277.
36. Lang R., Roth M., Stricker M. Development of a modular zeolite-water heat pump // *Proceeding of International Sorption Heat Pump Conference ISHPC 99*, Munich, Germany, 1999, pp. 611-618.
37. Nusselt W. Surface condensation of water vapour // *Z. Ver. Deut. Ing.*, 1916, Vol. 60, pp. 541-546 .

38. Glaznev I. S., Ovoshchnikov D. S., Aristov Yu. I. Kinetics of water adsorption under isobaric stages of adsorption heat pumps: the effect of isobar shape // *Intern. J. Heat &Mass Transfer*, 2008, (submitted).